Plasma Phys. Control. Fusion **41** (1999) A519–A529. Printed in the UK PII: S0741-3335(99)97501-2

Alfvénic turbulence associated with density and temperature filaments

G J Morales, J E Maggs, A T Burke and J R Peñano

Physics and Astronomy Department, University of California, Los Angeles, CA 90095, USA

Received 3 July 1998

Abstract. A systematic laboratory study of controlled density and temperature filaments having transverse scale length comparable to the electron skin-depth has been performed in the large plasma device (LAPD) at UCLA. It is found that large amplitude shear Alfvén waves develop spontaneously and are localized within the filaments. As the plasma conditions change (e.g., lowering the plasma beta parameter or increasing the heating power) the highly coherent eigenmodes develop into broad band Alfvénic turbulence. A kinetic description that includes the effect of coulomb collisions has been developed to understand the linear properties of the modes. Excellent agreement with the measured eigenfunctions is found for the density filaments in the higher beta regime in which the modes remain strongly coherent. The similarity between the broad band fluctuation spectra generated in a variety of plasma configurations suggest the possibility of a universal process involving filamentary structures and spontaneously generated Alfvénic turbulence.

1. Introduction

Measurements with high spatial resolution diagnostics developed over the past decade have shown that magnetized plasmas far from thermal equilibrium are filled with filamentary structures. The characteristic feature of filamentary structures is their great extent along the direction of the confining magnetic field as compared to their extent across the field. Transverse scale sizes of these structures are typically on the order of the electron skin-depth, c/ω_{pe}, or the ion Larmor radius, ρ_{i}, depending on the parameter ordering. Filamentary structures have been observed in a wide variety of plasmas, from naturally occurring space plasmas to laboratory and fusion device plasmas. They can consist of density depletions or enhancements, hot electron channels, localized currents or combinations thereof.

Rocket flights [1] and satellite observations [2] have documented that the auroral ionosphere is populated with filamentary density depletions within regions of extensive wave activity. Density filaments occur in regions where intense ion acceleration and suprathermal electron bursts are measured. Presently, there is a vigorous effort [3] aimed at understanding the role of Alfvén waves localized within auroral zone density filaments in the generation of energetic precipitating electrons. Filamentary density depletions have also been observed in an ionospheric high frequency (HF) heating experiment performed in Arecibo. *In situ* measurements [4] made by a rocket flying through field lines connected to the heated spot in the F-region of the ionosphere indicate that closely packed density depletions ($\delta n/n \approx 10\%$) having characteristic transverse scales between ρ_{i} and c/ω_{pe} are spontaneously generated during HF heating. There is also extensive evidence for the presence of filamentary structures in the solar and astrophysical environment. In fact, recent theoretical developments [5, 6]

0741-3335/99/SA0519+11$19.50

have pointed out the fundamental role played by c/ω_{pe} filaments in the reconnection processes which underly many space plasma phenomena.

There are two noteworthy experimental observations made in toroidal devices that illustrate the general nature of filamentary structures. Density filaments were imaged [7] under neutral beam heating conditions in the TFTR tokamak. These measurements demonstrated that large filamentary depletions ($\delta n/n \approx 50\%$) were spontaneously generated in a closed-packed arrangements (across B_0). In an experiment in the RTP toroidal device measurements made with a high-resolution Thomson scattering system identified [8] narrow electron temperature filaments ($\delta T_e/T_e \approx 50\%$) spontaneously generated during electron resonance heating conditions.

Filamentary structures with transverse scales of the order of c/ω_{pe} are particularly interesting because shear Alfvén waves develop parallel electric fields whose strength scales as $|E_\parallel| \approx (k_\perp c/\omega_{pe})(\omega/\omega_{pe})|\delta B_\perp|$ where ω is the wave frequency, $k_\perp$ the characteristic transverse wavenumber and $B_\perp$ is the transverse wave magnetic field. Hence, significant parallel electric fields can arise when $k_\perp c/\omega_{pe} \approx 1$. For instance, at fluctuating levels of $|\delta B_\perp|/B_0 \approx 10^{-3}$, under conditions of relevance to the auroral ionosphere, ambient electrons can gain roughly 1 keV of energy within one parallel wavelength. Correspondingly, for a tokamak environment an electron would gain an energy comparable to the loop voltage, thus a situation can be realized in which cross-field energy transport results without macroscopic mass transport.

Our group at UCLA has pursued detailed studies of controlled density [9, 10] and temperature filaments using the unique capability of the large plasma device [11] (LAPD). The material in this presentation emphasizes the properties of Alfvénic turbulence spontaneously generated in such structures and compares these observations to the turbulent behaviour at the plasma edge, a subject of considerable interest to studies of magnetic confinement. A contributed paper [12] at this conference uses analysis and particle simulation to examine the ion acceleration resulting from narrow layers driven by shear Alfvén waves. Recent studies by our group have also considered the structure of shear Alfvén waves of small transverse scale [13–15], the linear theory [16] of unstable eigenmodes trapped in density and temperature striations and the direct conversion [17] of whistler waves into electrostatic modes by density filaments. Perspectives of the laboratory studies for interpretations of spacecraft observations have also been presented [18, 19].

2. Laboratory device

The experiments reported here were conducted in the LAPD facility, a schematic of which is found at the top of figure 1. The plasma is generated by electrons (primaries) emitted from a heated, barium oxide coated cathode and subsequently accelerated by a semitransparent grid anode located 60 cm from the cathode. The accelerated primaries drift into a 9.4 m long vacuum chamber and strike neutral He gas at a fill pressure of 2×10^{-4} Torr to generate a He^+ plasma with greater than 75% degree of ionization. The end of the plasma column is terminated by an electrically floating copper plate, so no net current flows in the plasma region where the fluctuations are measured. The operating conditions used in the density filament studies are: uniform axial magnetic fields of 0.5–2 kG, axially uniform plasmas 45 cm in diameter with measured densities in the range $n \approx 1$–4×10^{12} cm^{-3}, electron temperatures $T_e \approx 5$–15 eV and ion temperatures $T_i \approx 0.1$–1 eV. The strength of the axial magnetic field is varied to attain different values of the electron plasma beta, $\beta_e = (m/M)(v_e/v_A)^2$, where m and M refer to the electron and ion mass, v_e is the electron thermal speed and v_A is the Alfvén speed.

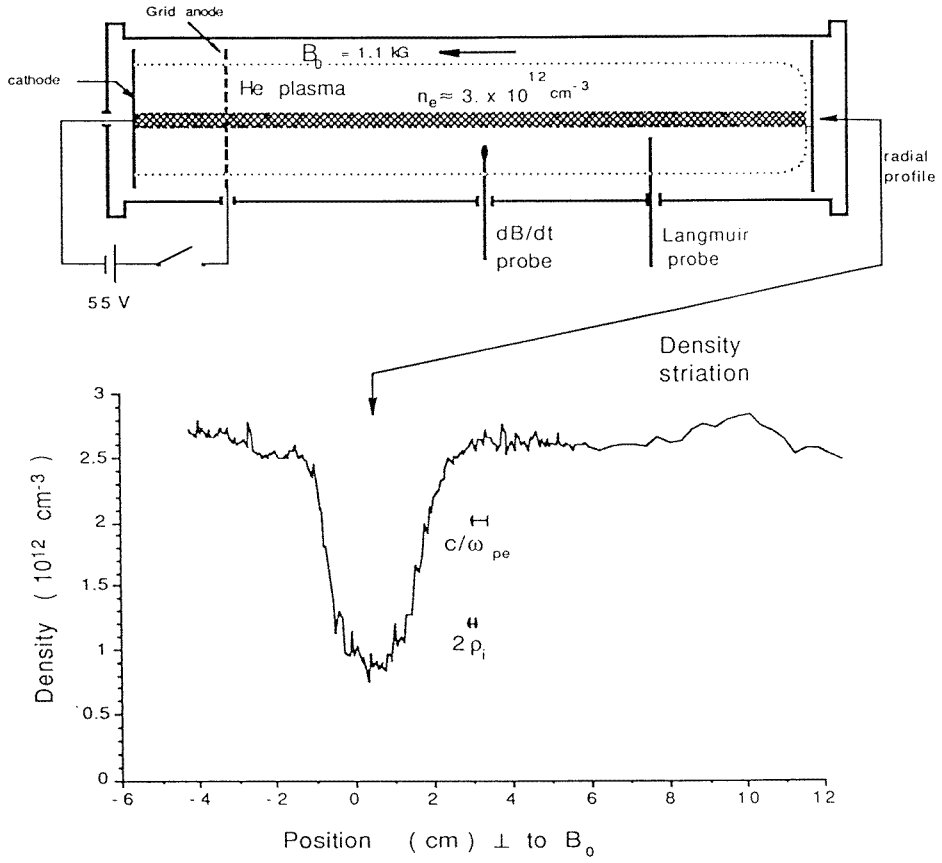

Figure 1. Experimental set up. Top: schematic of the plasma device (LAPD). Bottom: expanded view of the radial density profile of a controlled density filament whose axial extent is 10 m (the full length of the device).

3. Density filaments

Density filaments (or striations) consisting of regions of lower density than the surrounding plasma are generated by two methods. The most ideal consists of not applying the barium oxide coating to a small spot (≈1 cm radius) near the centre of the nickel cathode so that primaries are not emitted from this region. A more flexible method consists of placing a small copper disk supported on a long thin (2 mm diameter) ceramic shaft at a distance of 2 cm from a uniformly coated cathode. This technique results in filaments with properties nearly identical to those generated with the selective coating method.

The radial density profile of a typical density filament is shown at the bottom of figure 1. It should be noted that the plasma edge is located 20 cm from the centre of the filament. Thus, in the radial direction the filament can be considered to be embedded in an infinite plasma. Axially, it is found that the filament extends throughout the full length of the device. During the plasma discharge the electron temperature is also depressed within the filament. The electron temperature in the surrounding discharge plasma is $T_e \approx 10$–12 eV while $T_e \approx 6$ eV at the centre of the striation. Thus, a filament of reduced plasma pressure is produced in the discharge plasma within which large levels of low frequency (0.1–$0.3\omega_{ci}$) density and magnetic

fluctuations spontaneously develop (ω_{ci} is the ion gyrofrequency). For the results reported here $c/\omega_{pe} \approx 5$ mm, $\rho_i \approx 0.5$–2 mm and the ion sound gyroradius $\rho_s = (T_e/M)^{1/2}/\omega_{ci} \approx 2$–5 mm. Hence, the ordering of spatial scales is $L_N \geqslant L_T \approx c/\omega_{pe} \geqslant \rho_s > \rho_i$, where L_N and L_T are the density and temperature scale lengths.

4. Properties of spectra

The spontaneously generated magnetic field fluctuations, δB, are measured with a small induction loop probe consisting of mutually orthogonal coils in a triaxial arrangement. The fluctuations in density are obtained from the local ion saturation current, proportional to $n(T_e/M)^{1/2}$, collected by a small Langmuir probe. The local electron temperature is determined from the Langmuir probe current-voltage characteristic, but this measurement is not fast enough to correct for rapid fluctuations in T_e. Thus the signal we refer to as $|\delta n(\omega)|$ in subsequent figures may also contain contributions from fluctuations in T_e.

Figure 2 exhibits the correspondence between $|\delta n(\omega)|$ and $|\delta B(\omega)|$ near the steepest gradient region within the filament for two different values of plasma beta. Measurements of the polarization indicate that the magnetic fluctuations are shear Alfvén waves. Figure 2(a) corresponds to $\beta_e \approx 10^{-3} (> m/M)$ and demonstrates that excellent correspondence is obtained between peaks in the density and magnetic spectra, particularly in the lower range of frequencies $\omega/\omega_{ci} < 0.1$. In this higher β_e regime it is found from single-shot time traces that the oscillations in density and magnetic field are in phase. Since the polarization corresponds

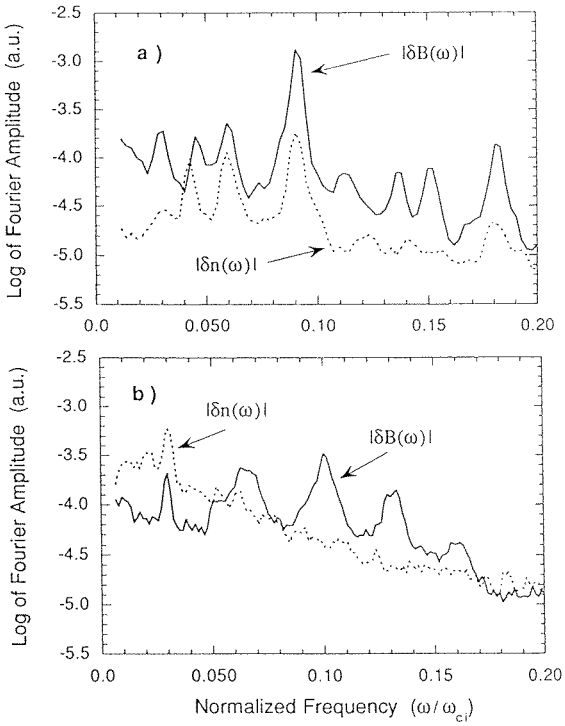

Figure 2. Frequency spectra of magnetic field fluctuations and density fluctuations within a density filament for two values of electron beta: (a) $\beta_e > m/M$ and (b) $\beta_e < m/M$.

to shear waves, these modes can be identified as drift-Alfvén waves that are trapped within the filament and are driven unstable by the density and temperature gradients. Figure 2(b) illustrates the behaviour obtained as β_e is lowered to $3 \times 10^{-4} (< m/M)$. It is seen that at this lower beta level the correspondence between the peaks in the density and magnetic spectra is limited to a small band of low frequencies, $\omega/\omega_{ci} < 0.03$. For these conditions clear peaks exist in the magnetic fluctuations at higher frequencies, $\omega/\omega_{ci} > 0.05$ where the density fluctuations exhibit an exponential frequency dependence with no semblance of an eigenmode structure.

The observed separation in mode structure that occurs as the value of β_e is changed can be understood from the theoretical boundaries shown in figure 3. The dark full curves correspond to theoretical calculations of the frequency of the fundamental eigenmode supported in the striation. The calculation [20] is based on a drift-kinetic description of the electron behaviour that includes pitch-angle collisions while the ion response follows cold fluid theory. The analysis is fully electromagnetic (includes shear and compressional modes) and automatically describes pure drift waves (region in curve 2 at large magnetic fields), pure Alfvén waves (curves 1 and 3), and drift-Alfvén waves (lower frequency region of curve 2 below 1.2 kG). The broken lines represent the smallest and largest values of the local Alfvén frequency within the pressure filament (i.e., $\omega = k_\parallel v_A$). The faint full curve merging with curve 2 corresponds to the results of purely electrostatic theory [16].

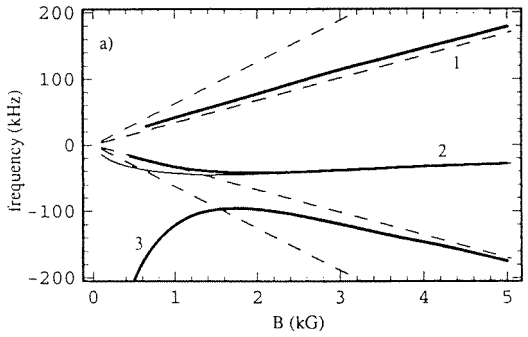

Figure 3. Theoretically predicted frequency of eigenmodes supported by a density filament for different magnetic field strengths. Broken curves correspond to the largest and lowest Alfvén frequencies within the filament.

Of all the various properties that we have measured the best theoretical understanding has been achieved in the prediction of the eigenfrequencies and radial eigenmodes of the lower frequency signals excited at higher beta ($> m/M$). An example is given in figure 4, in which the dark full curves correspond to the theoretically predicted eigenfunctions of density and magnetic field for the experimentally measured density and temperature profiles (broken curves with finite points through them). The full diamonds correspond to experimental measurements for the largest spectral peak. The predicted frequency of the eigenmode is 38 kHz and the observed value is 37 ± 2 kHz.

The magnitude of the observed fluctuations is $|\delta B|/B_0 \approx 10^{-3}$, a level which is consistent with limitation by convective nonlinearity, i.e. $k_\perp v_D \approx \omega$, where v_D is the $(E \times B)$ drift velocity due to a wave with perpendicular and parallel wavenumbers $k_\perp$ and $k_\parallel$. For a shear Alfvén wave this implies $|\delta B|/B_0 \approx (k_\parallel/k_\perp) \approx a/L \approx 10^{-3}$, the aspect ratio of the filament.

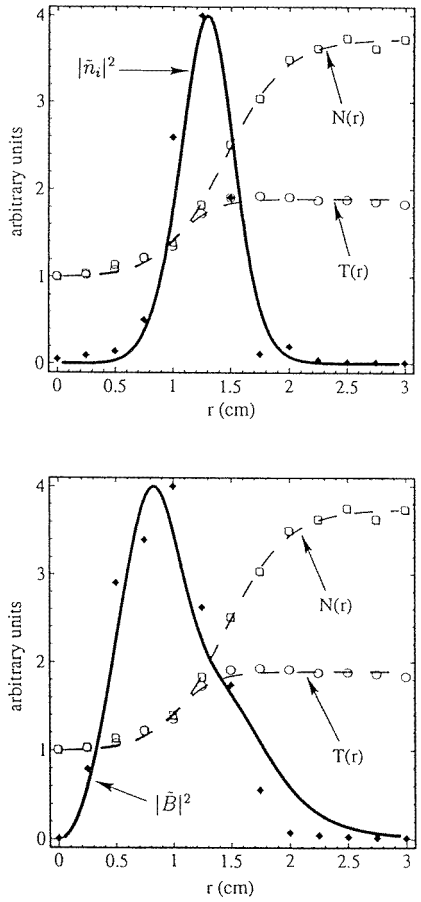

Figure 4. Theoretically predicted density and magnetic eigenfunctions (dark full curves) compared to experimental observations (full diamonds). Open symbols are measured density and temperature profiles of the filament. Broken curves are continuous profiles used in the theoretical calculations.

5. Edge turbulence

Figure 5 illustrates the typical behaviour in a background magnetic field of $B_0 = 1.1$ kG of the magnetic fluctuations (also having shear polarization), measured at the plasma edge (far from the density filament) at a position near the maximum edge density gradient. The top curve corresponds to a single-shot temporal signal and the bottom one to the ensemble average spectrum. The temporal signals indicate that the edge turbulence consists of impulsive events followed by a few cycles of clear oscillations. The associated spectrum exhibits a broad peak around 45 kHz (consistent with the lowest frequency of an axially standing shear Alfvén wave) followed by a nearly exponential decay at higher frequencies. The correspondence between the spectrum of magnetic and density fluctuations at the plasma edge is shown in figure 6. The density spectrum peaks toward low frequencies and exhibits a clear exponential decay over the frequency range where the magnetic fluctuations have a peak. This behaviour is analogous to that observed within a density filament at large background magnetic fields (i.e., lower β_e). This feature is emphasized by comparing figure 6 with figure 7, which displays the spectrum

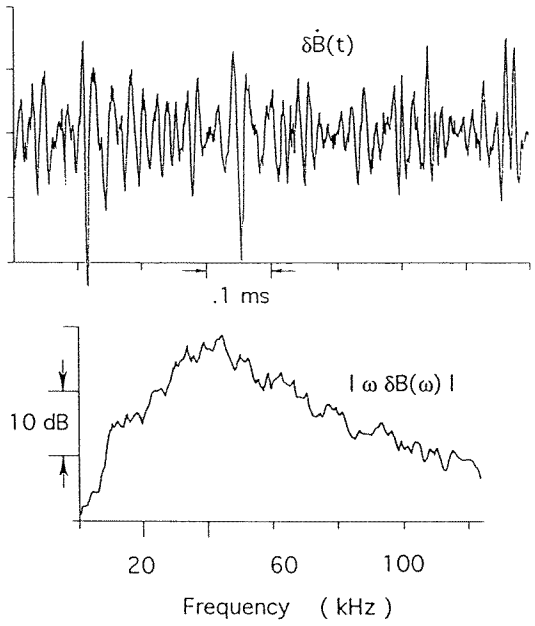

Figure 5. Single-shot temporal behaviour and frequency spectrum (ensemble average, log scale) of the time derivative of the magnetic field fluctuations at the plasma edge (far from the density filament).

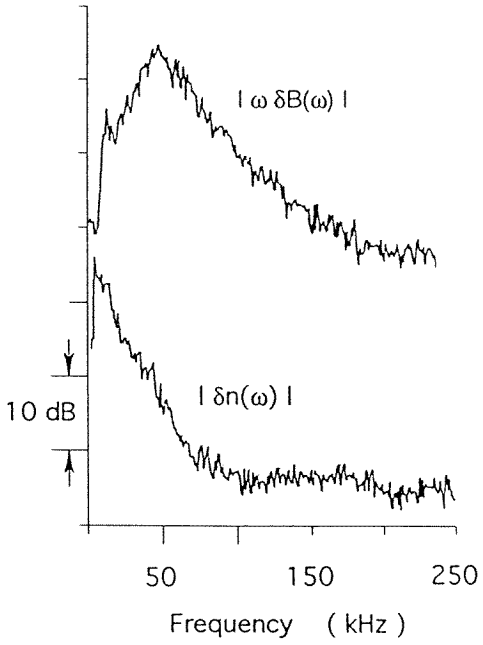

Figure 6. Frequency spectrum of density fluctuations at the plasma edge compared to the frequency spectrum of the time derivative of the magnetic field fluctuations (log scale).

within a density filament at 2 kG. The broad-band nature of the Alfvénic turbulence is nearly identical to that at the plasma edge, except for the presence of a discrete set of eigenmodes.

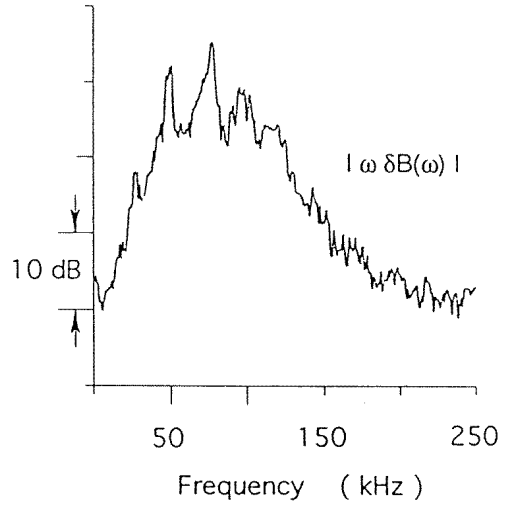

Figure 7. Frequency spectrum (log scale) of the time derivative of magnetic fluctuations within a density filament for $\beta_e < m/M$. To be compared to figure 6.

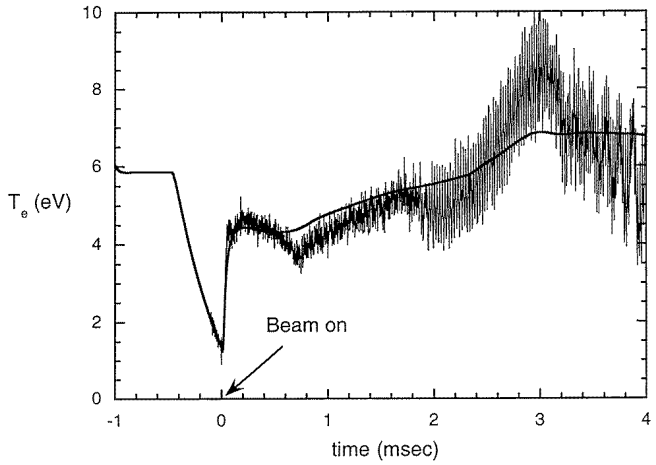

Figure 8. Time evolution of electron temperature at the centre of a temperature filament. Full curve is prediction of two-dimensional (2D) classical heat transport code. Noisy curve is experimental observation.

6. Temperature filaments

The temporal evolution of narrow temperature filaments with transverse scale sizes on the order of c/ω_{pe} is investigated during the afterglow phase of the plasma, i.e. after the discharge voltage pulse is terminated. In the afterglow plasma T_e decays rapidly (on a time scale of 100 μs), but the plasma density decays slowly (on a scale of 2 ms). Temperature filaments are generated by a heat source consisting of a small electron beam 3 mm in diameter produced by biasing a heated, single crystal of lanthanum hexaboride to a low voltage (typically 20 V which results in an injected current of 200 mA). The beam injector is located 75 cm from

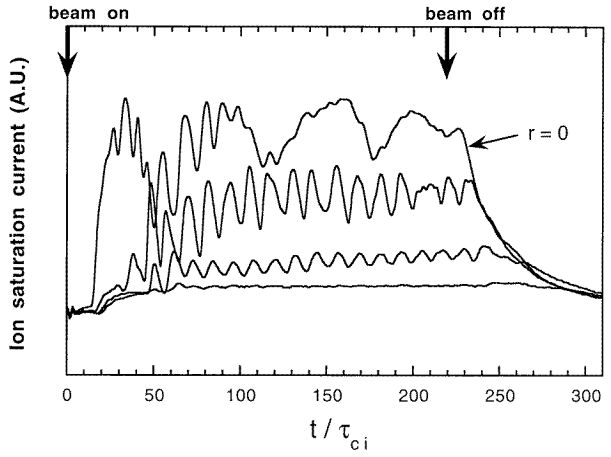

Figure 9. Example of highly coherent fluctuations that spontaneously develop in a temperature filament. Shown is the time evolution (scaled to $2\pi/\omega_{ci}$) of ion saturation current for different radial positions within a narrow temperature filament generated by a short-pulse beam.

the end of the plasma column (see figure 1 for orientation). The beam electrons slow down and transfer their energy to the cold background plasma at a distance of about 1 m. From this extended heat source simultaneous axial and radial thermal conduction creates an expanding temperature filament which spontaneously develops magnetic, density and temperature fluctuations.

Figure 8 shows the time evolution of the electron temperature at the centre of the thermal plume at an axial position 285 cm away from the beam injector. The smooth full curve is the theoretically predicted classical behaviour (due to Coulomb collisions) and the noisy curve is the experimental result. For time scales less than 2 ms the prediction of classical theory is excellent, however, as the plume develops steeper gradients and reaches higher temperatures, oscillations in the ion saturation current develop at a frequency of about $0.1\,\omega_{ci}$. In addition, large amplitude fluctuations at lower frequency (about $0.02\,\omega_{ci}$) appear around 3 ms after beam turn-on. The higher frequency modes are radially localized in the gradient regions of the plume and are similar in nature to the drift-Alfvén waves that grow in density filaments. The low-frequency modes are confined to the central region of the plume and resemble ion acoustic waves. It is evident from figure 8 that after the onset of fluctuations, significant departures from classical heat transport develop. First, after onset of high-frequency oscillations, the central temperature rises faster than the classical prediction and then rapidly decreases after onset of low-frequency oscillations.

Under certain conditions temperature filaments can develop extremely coherent fluctuations, in a manner analogous to the sharp eigenmodes that grow at higher β_e in density filaments. Figure 9 displays the time evolution of the ion saturation current at three radial positions for a short-pulse beam. The traces correspond to 20-shot averages thus indicating the remarkable coherency of the phenomena. Detailed measurements in the plane perpendicular to B_0 (not shown) have uncovered that the high-frequency oscillations are spiral waves. Temperature filaments can also develop broad band Alfvénic turbulence, as is indicated in figure 10 for three different values of the beam voltage. It is evident that the magnetic spectra generated under these conditions is nearly identical to that observed at the plasma edge (figure 6) and within density filaments at the lower β_e values (figure 7), thus strongly suggesting universal behaviour.

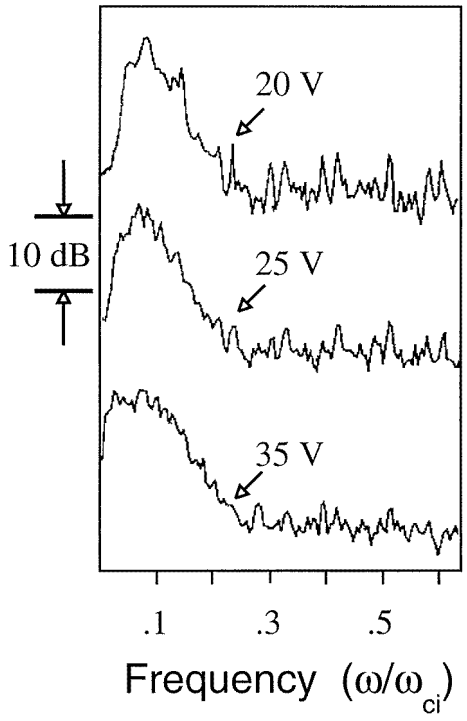

Figure 10. Example of broad band Alfvénic turbulence that develops in temperature filaments. Shown is the spectrum of the time derivative of magnetic field fluctuations (log scale) for filaments generated by beams of different voltage. To be compared to the behaviour at the plasma edge (figure 6), and within a density filament (figure 7).

7. Conclusions

In non-thermal plasmas, filamentary structures with transverse scale sizes on the order of c/ω_{pe} spontaneously generate Alfvénic turbulence spatially localized to the filament region. The properties of the fluctuations generated by the plasma non-uniformities associated with the filamentary structures depend upon the value of the electron plasma beta; ranging from drift-Alfvén waves at high beta ($>m/M$) to pure shear Alfvén waves at low beta ($<m/M$) plasmas. The similarity between the fluctuation spectra generated in a variety of plasma configurations (such as the plasma edge and density striations) suggest the possibility of a universal process involving filamentary structures and spontaneously generated Alfvénic turbulence.

Acknowledgments

The work of GJM and JRP is sponsored by USDOE and ONR, that of JEM by ONR and NSF, and ATB by ONR. The LAPD facility was developed by Professor W Gekelman.

References

[1] Kintner P M, Vago J, Chesney S, Arnoldy R L, Lynch K A, Pollock C J and Moore T E 1992 *Phys. Rev. Lett.* **68** 248

[2] Stasiewicz K, Gustafsson G, Marklund G, Lindqvist P.-A, Clemmons J and Zanetti L 1997 *J. Geophys. Res.* **102** 2565

[3] A report of the first study group meeting at the International Space Science Institute in Bern, Switzerland available at http://tatra.irfu.se/ks/www/research/issi/.
[4] Kelley M C, Arce T L, Salowey J, Sulzer M, Armstrong W T, Carter M and Duncan L 1995 *J. Geophys. Res.* **100** 17 367
[5] Drake J F, Kleva R G and Mandt M E 1994 *Phys. Rev. Lett.* **73** 1251
[6] Kleva R G 1994 *Phys. Rev. Lett.* **73** 1509
[7] Zweben S J and Medley S S 1989 *Phys. Fluids* B **1** 2058
[8] Lopes Cardozo N J, Schuller F C, Barth C J, Chu C C, Pipjer F J, Lok J and Oomens A A M 1994 *Phys. Rev. Lett.* **73** 256
[9] Maggs J E and Morales G J 1997 *Phys. Plasma* **4** 290
[10] Maggs J E and Morales G J 1996 *Geophys. Res. Lett.* **23** 633
[11] Gekelman W, Pfister H, Lucky Z, Bamber J, Leneman D and Maggs J 1991 *Rev. Sci. Instrum.* **62** 2875
[12] Reitzel K J and Morales G J 1998 Dynamics of narrow electron streams in magnetized plasmas *ICPP 1998* Prague, poster p 2.142
[13] Morales G J, Loritsch R S and Maggs J E 1994 *Phys. Plasmas* **1** 3765
[14] Morales G J and Maggs J E 1997 *Phys. Plasmas* **4** 4118
[15] Gekelman W, Leneman D, Maggs J and Vincena S 1994 *Phys. Plasmas* **1** 3775
[16] Peñano J R, Morales G J and Maggs J E 1997 *Phys. Plasmas* **4** 555
[17] Bamber J F, Gekelman W and Maggs J E 1994 *Phys. Rev. Lett.* **73** 2990
[18] Maggs J E, Morales G J and Gekelman W 1997 *Phys. Plasmas* **4** 1881
[19] Bamber J F, Maggs J E and Gekelman W 1995 *J. Geophys. Res.* **100** 23 795
[20] Peñano J R 1997 Fluctuations associated with plasma density and temperature striations *PhD Thesis* University of California, Los Angeles (December 1997)